A Letters Journal Exploring the Frontiers of Physics

January 2011

EPL, **93** (2011) 16004
doi: 10.1209/0295-5075/93/16004

www.epljournal.org

Anchoring transition in confined discotic columnar liquid crystal films

Thomas Brunet, Olivier Thiebaut, Émilie Charlet, Harald Bock, Julien Kelber and Éric Grelet[a]

Centre de Recherche Paul-Pascal, CNRS-Université de Bordeaux - 115 Avenue Schweitzer, 33600 Pessac, France, EU

received 15 November 2010; accepted in final form 22 December 2010
published online 1 February 2011

PACS 61.30.Hn – Surface phenomena: alignment, anchoring, anchoring transitions, surface-induced layering, surface-induced ordering, wetting, prewetting transitions, and wetting transitions
PACS 64.70.mj – Experimental studies of liquid crystal transitions
PACS 68.55.-a – Thin film structure and morphology

Abstract – We report the achievement of ultrathin films (down to 25 nm thick) of thermotropic columnar liquid crystals in homeotropic alignment (columns normal to the interface) confined between a glass slide and a thin metallic electrode (about 150 nm thick). The face-on orientation of the discotic compound is obtained by anchoring transition of a columnar liquid crystalline phase from a degenerate planar orientation to the homeotropic alignment without any phase transition to the isotropic liquid phase. The kinetic dependence on temperature of such anchoring transition is investigated revealing various diffusive growth regimes of the homeotropic domains. Finally, confining effects are also considered by varying the thickness of the columnar liquid crystal film to reach the typical value required in organic solar cells thus demonstrating the reliability of such alignment process in a photovoltaic context.

Introduction. – Columnar liquid crystals (CLCs) formed by discotic molecules are known to exhibit high charge mobilities and large exciton diffusion lengths along the column direction providing promising applications in organic electronics [1–3]. Such properties stem from the overlapping of π-orbitals of adjacent discotic molecules inside a column, providing a one-dimensional pathway for charge migration. Thus, CLCs can be used as active layers in optoelectronic devices if the columnar stacks are properly aligned between electrodes. For solar cells [4], the homeotropic alignment (columns normal to the interface) is required to benefit from efficient electronic properties in the mesophase [5]. Highly ordered homeotropically aligned thin films have been successfully obtained in open films of about 200 nm thick by controlling the growth kinetics of the columnar domains during thermal annealing [6]. The use of a polymer sacrificial layer has been also proposed to induce the homeotropic alignment [7]. Recently, the first proof of principle of an organic heterojunction based on two oriented columnar liquid crystal layers has been reported [8]. However, when the film thickness is further reduced to the typical value required in organic solar cells, *i.e.* 25–100 nm [9] considering the light absorption coefficients *vs.* the exciton diffusion length [10] and the charge carrier mobility [11], the homeotropic alignment is increasingly disfavored over the planar orientation and dewetting may occur leading then to strongly inhomogeneous films and therefore short-circuits inside the photovoltaic device. Nevertheless, the achievement of uniform ultrathin films has been recently reported down to 50 nm thick in the geometry of open supported films on indium tin oxide (ITO) cathode [12]. As the homeotropic alignment is favored by solid-CLC interfaces [6,13], the deposition of a second electrode on CLC films would favor to the face-on orientation. However, it is far from obvious that thin metallic electrodes used in photovoltaic devices —typically 100 nm thick [14]— play the role of a macroscopic solid interface. We address this question by presenting new experimental results on the anchoring transition of a CLC phase from a degenerate planar orientation to the homeotropic alignment (fig. 1). The phenomenon of anchoring transition where the liquid crystal orientation can be tuned between two different alignments without any phase transition has been studied in a few systems, from thermotropic nematic to lyotropic chromonic mesophases [15–17]. In this work we used a discotic columnar liquid crystal confined between a glass slide —with or without ITO— and a thin silver layer.

[a] E-mail: grelet@crpp-bordeaux.cnrs.fr

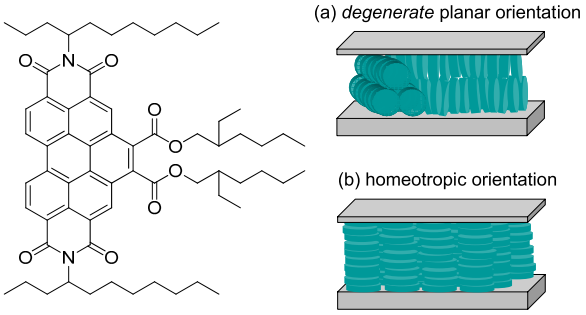

Fig. 1: (Colour on-line) Left: molecular structure of the discotic material studied in this paper, which is a benzoperylene derivative. The main feature of this compound is to exhibit a hexagonal columnar liquid crystalline phase at ambient temperature. Right: schematic representation of the different orientations of a columnar liquid crystal: *degenerate* planar (a) and homeotropic (b) orientations.

The alignment process consists in a thermal annealing of the CLC films well below the clearing temperature of the discotic compound. For such temperatures, the decrease of its viscosity allows internal reorganizations occurring within the mesophase and then leads to a change in the orientation of the columnar domains [18]. Thus, we show that ultrathin CLC films (down to 25 nm in thickness) of a hexagonal columnar mesophase can be stabilized in homeotropic orientation by this alignment process.

Material and methods. – The discotic material used here is a benzoperylene derivative (fig. 1) which has been synthesized following a published procedure [19]. Its phase behavior features a hexagonal columnar liquid crystalline (CLC) phase from ambient temperature to the isotropic liquid phase (Iso) at $T_{CLC\text{-}Iso} = 152\,^{\circ}\mathrm{C}$. The liquid crystal solution of a few wt% in *n*-heptane is spin-coated at 2000 rpm during 30 seconds on cleaned glass slides. The substrates without ITO have been dipped into sulfochromic acid and rinsed with distilled water beforehand. In the case of ITO substrates, they are preliminarily cleaned with three successive ultrasonic baths of 10 min each, of acetone, methanol, and isopropanol. A surface treatment is then applied on the ITO electrode by UV-ozone [12], with a commercial ultraviolet ozone cleaning system (UVOCS, USA) during a period of 30 min. Finally, the silver layer is deposited on the CLC films thanks to a thermal evaporator (Edwards Auto 306) characterized by a long sample-metal source distance (20 cm). The thickness of the silver layer (typically 150 nm) and the speed of deposition (0.1 Å/s to 1 Å/s) are accurately determined by a 6 MHz quartz crystal microbalance positioned close to the sample. Silver exhibits a purity of 99% and is furnished by Sigma Aldrich. The CLC film thicknesses —ranging from 500 nm down to 25 nm— are measured by using an atomic force microscope in tapping mode acting as a mechanical profilometer.

The orientation of the CLC films is studied by polarizing and differential interference contrast (DIC) microscopy in reflection mode using the silver layer as light reflecting substrate.

Results. – Just after the silver deposition, the confined CLC film exhibits a birefringent mosaic texture (fig. 2(a)) characteristic of a powder, as shown by X-ray scattering measurements (see fig. 3(a)). This optical texture is similar to the one obtained after spin-coating for an open CLC film [20]. It corresponds to a *degenerate* planar orientation for which columnar domains of about a few μm in size are in the plane of the substrate but oriented in different directions (fig. 1(a)), as recently shown in a previous study by grazing X-ray diffraction [20].

In a first step, the CLC film is heated up to $T = 100\,^{\circ}\mathrm{C}$, *i.e.* well below the clearing point of the bulk liquid crystal ($T_{CLC\text{-}Iso} = 152\,^{\circ}\mathrm{C}$). Two hours later, the heterogeneous nucleation and the growth of non-birefringent hexagonal germs have occurred (fig. 2(b)). These sixfold symmetric domains remain by cooling the sample down to room temperature (fig. 2(c)). If the sample is then heated at higher temperature, *e.g.* up to $T = 120\,^{\circ}\mathrm{C}$, the growth of the non-birefringent domains restarts but germs become ribbed (fig. 2(d)). A few tens of minutes later, the whole CLC film becomes non-birefringent, and remains in this state after cooling down at ambient temperature, as proven by fig. 2(e).

Although a premature phase transition from the columnar liquid crystalline phase to the isotropic liquid phase could be invoked, a confinement-induced down-shift of the clearing temperature by $\sim 50\,^{\circ}\mathrm{C}$ seems unrealistic. In addition, the lack of birefringence is retained at room temperature, ruling out the assumption of an isotropic liquid state. Here, this optical feature is characteristic of homeotropic anchoring, where the column orientation —corresponding to the optical axis of the liquid crystal— coincides with the direction of light propagation perpendicular to the substrate. Thus, there is no optical anisotropy detectable by polarizing microscopy. Moreover, the sixfold symmetry of germs is an additional signature of homeotropic alignment of the hexagonal columnar mesophase. The homeotropic anchoring being thermodynamically stable at room temperature, the reliability of such alignment process in order to achieve face-on orientation of confined CLC films is proven. Although the silver electrode is very thin, this metallic layer still succeeds in playing the role of a solid interface.

Such a homeotropic alignment has been confirmed by synchrotron X-ray scattering, which was performed on the BM02 beamline at ESRF (Grenoble, France) at high energy (15.9 keV) to improve sample transmission[1]. Figure 3 shows the X-ray diffraction pattern obtained

[1]The transmission of the sample is weak due the absorption of both the glass slide and the silver layer. That is why these X-ray diffraction measurements have been performed on the thickest CLC film we consider here ($\delta_{CLC} \sim 500$ nm) covered by an ultrathin silver layer ($\delta_{Ag} \sim 50$ nm) in order to improve the signal-to-noise ratio. The sample-to-detector distance was 16 cm, and the X-ray beam had a size of $200 \times 350\,\mu\mathrm{m}^2$.

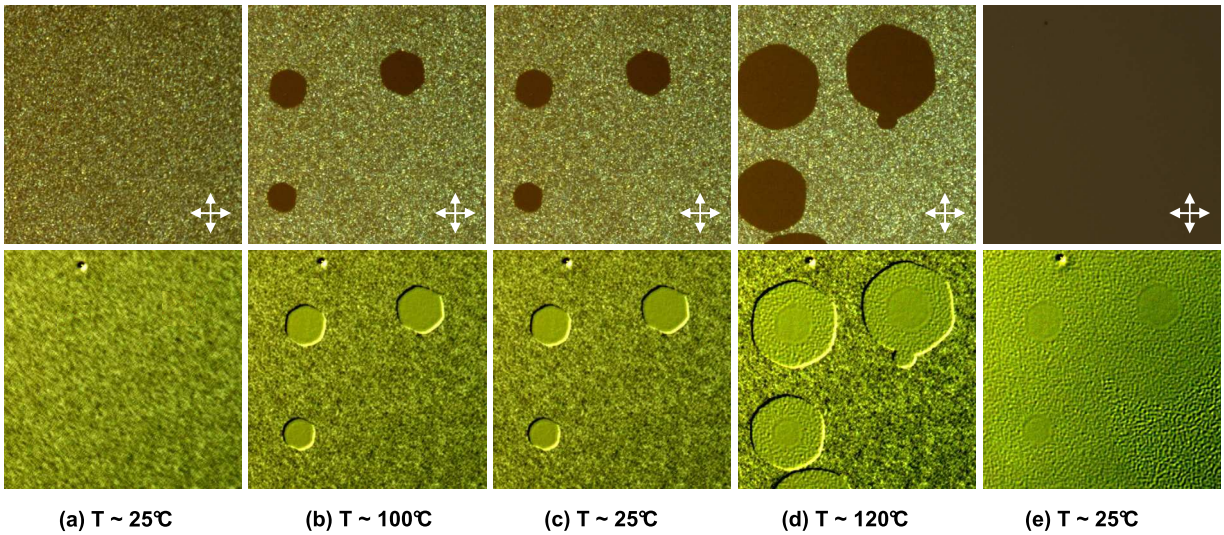

Fig. 2: (Colour on-line) Growth by anchoring transition of homeotropically oriented domains studied for a CLC film (150 nm thick) confined between a glass plate and a thin silver layer (150 nm thick). Optical observations between crossed polarizers (top) and by differential interference contrast microscopy (bottom). The image size is $350\,\mu\text{m} \times 350\,\mu\text{m}$. (a) At room temperature, *i.e.* $T = 25\,^{\circ}\text{C}$, the CLC film exhibits a birefringent mosaic texture characteristic of a powder. Then, two successive thermal cycles are applied to the sample. The first one consists in a temperature increase up to $T = 100\,^{\circ}\text{C}$. (b) After two hours at this temperature, non-birefringent hexagonal germs have developed. (c) The sample is quickly cooled down to room temperature $T = 25\,^{\circ}\text{C}$. (d) The sample is heated again up to $T = 120\,^{\circ}\text{C}$. After half an hour at such temperature, the germ growth has restarted but destabilizations occur within the CLC film as illustrated by its ribbed texture observed by DIC microscopy. (e) After one hour at $T = 120^{\circ}\text{C}$, the whole sample becomes irreversibly non-birefringent as illustrated by pictures taken after cooling down at room temperature ($T = 25\,^{\circ}\text{C}$).

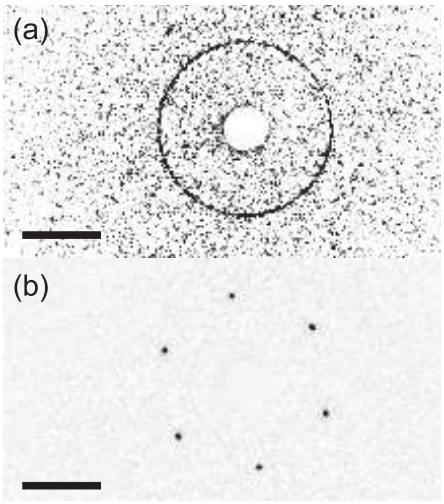

Fig. 3: X-ray diffraction pattern observed in the geometry of confined CLC films (500 nm thick) between a glass slide and a thin silver layer (50 nm thick) investigated in transmission. The scale bar indicates $3\,\text{nm}^{-1}$. (a) Powder-like oriented sample and (b) single homeotropically oriented CLC domain obtained after the anchoring transition. The sixfold symmetry is the signature of homeotropic alignment of the hexagonal columnar mesophase.

for a sample before (fig. 3(a)) and after (fig. 3(b)) the anchoring transition, which corresponds to a powder-like (as in fig. 2(a)) and a homeotropically oriented (as in fig. 2(e)) CLC layer, respectively. The six-fold symmetry observed in fig. 3(b) demonstrates the face-one columnar orientation, which is developed over large areas.

For comparison, the homeotropic alignment has been also obtained by heating up the sample with the metallic electrode *beyond* the clearing temperature ($T_{CLC\text{-}Iso}$) in order to achieve very thin homeotropically oriented films [12]. The phase transition into the isotropic liquid phase induces strong inhomogeneities within the film (figs. 4(a)–(c)). By cooling down the sample, the columnar mesophase nucleates at $T = 148\,^{\circ}\text{C}$ (fig. 4(d)), with the growth of a hexagonal germ —characteristic of face-on orientation— expanding all over the sample (fig. 4(e)). The comparison between fig. 4(a) and fig. 4(e) where some destabilization of the sample occurred shows unambiguously that anchoring transition turns out to be more appropriate in order to achieve homogeneous homeotropically oriented films than the thermal process with the isotropization step.

In this work, the influence of the heating temperature on the kinetics of the anchoring transition is quantitatively explored (figs. 5(a), (b)). Let us consider a typical thickness value required in organic solar cells, *e.g.* $\delta_{CLC} = 50\,\text{nm}$. If the confined CLC film is progressively heated up from room temperature, we note that the anchoring transition is activated at $T = 80\,^{\circ}\text{C}$ since non-birefringent germs nucleate at this temperature. By maintaining the temperature constant, the time-evolution of the germ radius R is then measured by differential interference contrast microscopy (fig. 5(a)). First, we

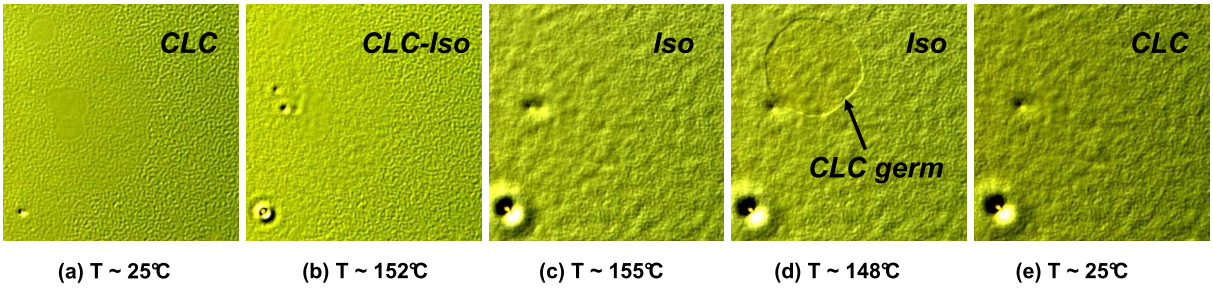

Fig. 4: (Colour on-line) Evolution with temperature of the previous homeotropically oriented CLC film (150 nm in thickness) confined between a glass slide and a thin silver layer (150 nm in thickness), presented in fig. 2(e). The optical observations are done by DIC microscopy. Each image has a size of $350\,\mu\text{m} \times 350\,\mu\text{m}$. (a) At room temperature, the sample is ribbed because of the fast anchoring transition previously achieved at $T = 120\,^{\circ}\text{C}$, see fig. 2(e). (b) At $T \sim 152\,^{\circ}\text{C}$ corresponding to the clearing point ($T_{CLC\text{-}Iso}$), strong inhomogeneities appear around the defect suggesting a transition to the isotropic liquid phase. (c) At $T = 155\,^{\circ}\text{C}$, the discotic film in isotropic liquid phase is destabilized. (d) By cooling the sample down to the room temperature, the columnar liquid crystalline phase nucleates at $T = 148\,^{\circ}\text{C}$ as indicated by the sixfold symmetry of the germ. (e) At room temperature, *i.e.* $T = 25\,^{\circ}\text{C}$, the irreversible destabilization of the sample due to the isotropization step is clearly evidenced.

observe a transient regime during which R increases as $\sqrt{t}$ followed by a permanent one during which R is a linear function of t. In this latter regime, we are able to extract the growth velocity V of homeotropic germs from the time measurements $R(t)$ that is found to be about $V = 0.1\,\mu\text{m/min}$ at $T = 80\,^{\circ}\text{C}$. For such slow anchoring transition, the homeotropic domains develop homogeneously as indicated by the smooth texture of the hexagonal germ shown in the inset of fig. 5(a). If the heating temperature is much higher, *e.g.* $T = 120\,^{\circ}\text{C}$, the homeotropic germs develop circularly as illustrated in the inset of fig. 5(b). Moreover, their growth is much faster: $V \sim 40\mu\text{m/min}$ at $T = 120\,^{\circ}\text{C}$. However, this fast anchoring transition provides ribbed homeotropic germs as illustrated in the inset of fig. 5(b) and leads to inhomogeneous oriented CLC films.

The various growth regimes observed may be discussed on the base of previous works reported on the free growth of a hexagonal columnar liquid crystal in coexistence with its isotropic liquid phase [21]. It is important to note that these previous works deal with a *phase transition*. Our work here is about an *anchoring transition* occurring in the same columnar liquid crystalline phase. Nevertheless, we note many surprising similarities between these two phenomena that will be presented in the two following paragraphs.

The feature illustrated in fig. 5(a) has been already observed by Oswald *et al.* [22]: a first growth regime in $\sqrt{t}$ and then a second one at constant velocity. The authors pointed out a morphological transition between two diffusive growth regimes: the *petal-shape* regime and the *dendritic* regime. The germ, circular at the beginning, destabilizes above a certain radius and a hexagonal modulation develops which is amplified by the destabilizing effect of the diffusion field [23]. Then, the petals glide into six independent *dendrites* [24]; their tips move at constant velocity $V = \text{d}R/\text{d}t$. In both regimes, the germs exhibit a hexagonal envelope as we observe in our experiments (inset of fig. 5(a)). Unfortunately, optical microscopy does not allow us to explore the mesophase at such small scale to evidence the dendrites.

A second morphological transition has been observed at larger velocities between the *dendritic* regime and a third diffusive growth regime called *dense-branching* regime [22]. If such transition is still difficult to explain, the authors have attributed the destabilization of the initial hexagonal pattern into a circular one "to the development of the sidebranching and to the tip-splitting of the six primary dendrites". Such a mechanism could be reasonably invoked in our experiments because of the circular shape of the homeotropic domains growing at high temperature (inset of fig. 5(b)). In addition the ribbed structure of germs we observed remind the shape of the new dendrites which are formed with the sidebranching of the six main dendrites in the *dense-branching* regime. Once again, these structures are unfortunately not observable in our experiments by optical microscopy.

Thus, the detailed mechanism of the different growth regimes appearing during the anchoring transition has still to be elucidated. The origin of the supersaturation which is chemical or thermal for the growth regimes during a phase transition [21] remains unclear in the case of the anchoring transition. An assumption could be that the homeotropic and planar regions behave as two distinct thermodynamic phases because 1) the homeotropic orientation is energetically favored for surface tension considerations [6] especially in this geometry of thin films, 2) the planar region is formed by a multitude of small domains of a few μm in size, with therefore the presence of a high density of grain boundaries. The impurity segregation involved by the diffusion field taking place at the interface of the growing domains could then mainly be located in the core of many defects being in between the planar domains.

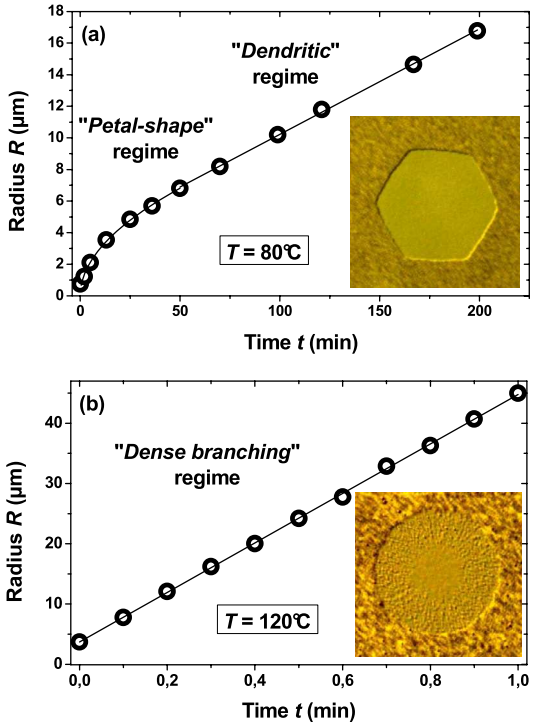

Fig. 5: (Colour on-line) Time-evolution of the radius R of homeotropic germs growing by anchoring transition. The CLC film and the silver layer are about 50 nm and 150 nm thick, respectively. (a) At $T = 80\,^{\circ}$C, the growth is first in $\sqrt{t}$ suggesting a *petal-shape* regime; then, the hexagonal germ radius R increases linearly with time t, a characteristic feature of the *dendritic* regime. (b) At $T = 120\,^{\circ}$C, the homeotropic germ also develops at constant velocity $V = \mathrm{d}R/\mathrm{d}t$ but circularly. Moreover, this oriented domain becomes ribbed suggesting a *dense-branching* regime. Optical observations showed in the insets are performed by DIC microscopy and the image size is $250\,\mu\mathrm{m} \times 250\,\mu\mathrm{m}$.

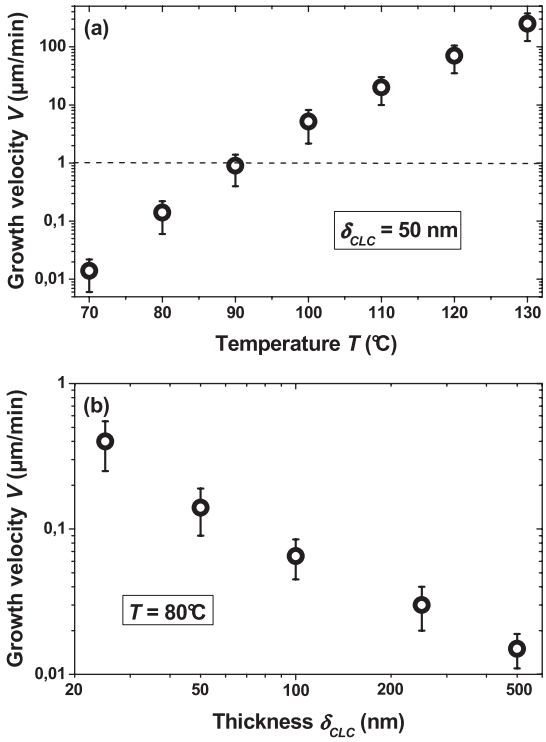

Fig. 6: Growth velocity V of the homeotropic germs within confined CLC films, covered by a 150 nm thick silver layer, as a function of (a) the heating temperature T for $\delta_{CLC} = 50$ nm (semi-log scale) and (b) the CLC film thickness δ_{CLC} for $T = 80\,^{\circ}$C (log-log scale). The dashed line refers to the threshold between a stable germ growth in the *dendritic* regime and a ribbed germ growth in the *dense-branching* regime (see the text).

In this paper, we characterize quantitatively the growth velocity V of homeotropic germs by measuring the time-evolution of their radius for various heating temperature ranging from $T = 70\,^{\circ}$C up to $T = 130\,^{\circ}$C (see footnote [2]). A drastic dependence on the heating temperature T of the growth velocity V is evidenced over five decades as illustrated in fig. 6(a) presented in the semi-log scale. According to our optical microscopy observations, homeotropic germs become ribbed from about $T = 90\,^{\circ}$C, corresponding to $V \sim 1\,\mu$m/min. Above such growth velocity, the CLC film is more or less destabilized depending on the heating temperature. Therefore, it is essential to accurately control the kinetics of the anchoring transition. In a context of solar cell elaboration, strong inhomogeneities within the CLC films could lead to short-circuits inside the photovoltaic device and have then to be avoided.

[2]Note that for the growth velocity measurment at $T = 70\,^{\circ}$C, the anchoring transition has been initially activated at $T = 80\,^{\circ}$C before a cooling down of the sample to $T = 70\,^{\circ}$C.

We also investigate qualitatively the influence of the electrode thickness, δ_{Ag}, on the anchoring transition, which is observed from $\delta_{Ag} = 150$ nm (the usual electrode thickness used in photovoltaic devices [14]) down to 15 nm. Thus, a metallic cathode of only 15 nm thick still behaves as a macroscopic solid interface for the CLC orientation. Finally, the effect of the CLC film thickness δ_{CLC} —ranging from 500 nm down to 25 nm— on the kinetics of anchoring transition in the *dendritic* regime is quantitatively studied. As explained above, it is necessary to proceed at sufficient low heating temperature —*e.g.* $T = 80\,^{\circ}$C— in order to achieve homogeneous oriented structures. As shown in fig. 6(b), the thinner the confined CLC film is, the faster the anchoring transition occurs. This latter result is of great interest in a context of photovoltaic device manufacturing: thin oriented CLC films of about 50 nm thick are expected to be more efficient than thicker ones because of the exciton diffusion length which has been found to be up to 70 nm in CLC-based devices [10]. Thus, we show here that an anchoring transition is an appropriate alignment process for CLC films of about 50 nm in thickness, where the heating temperature can be easily adjusted to quickly induce the CLC reorientation without destabilization of the sample.

In conclusion, we report an efficient alignment process —anchoring transition— in order to achieve face-on orientation of columnar liquid crystal films. This technique appears useful to obtain easily a homeotropically oriented discotic material in the range of thicknesses required for photovoltaic devices (about 50 nm in thickness) by taking benefit from a direct contact with the thin metallic electrode (about 150 nm in thickness). Thus, it could provide a feasible alternative regarding to more thickness-sensitive alignment processes recently proposed [12]. However, we demonstrate that it is necessary to precisely control the kinetics of the anchoring transition: a critical growth velocity of homeotropically oriented domains of about $1\,\mu$m/min should not be exceeded because of strong inhomogeneities developing within the CLC film. This alignment process provides new opportunities to develop face-on oriented bilayers of two discotic columnar liquid crystals for organic donor-acceptor heterojunction devices.

* * *

This research was supported by the CNRS, ANR grants, and GIS Advanced Materials in Aquitaine. We thank C. Rochas from the BM02 beamline at ESRF (Grenoble, France) for his help in synchrotron experiments. Author contributions: EG designed research; EC did the preliminary experiments; HB and JK synthesized the discotic compound; OT and TB prepared the samples and performed the optical microscopy experiments; EG performed the X-ray scattering experiments; TB analyzed data; TB and EG wrote the paper.

REFERENCES

[1] Laschat S., Baro A., Steinke N., Giesselmann F., Hagele C., Scalia G., Judele R., Kapatsina E., Sauer S., Schreivogel A. and Tosoni M., *Angew. Chem., Int. Ed.*, **46** (2007) 4832.
[2] Sergeyev S., Pisula W. and Geerts Y. H., *Chem. Soc. Rev.*, **36** (2007) 1902.
[3] Pisula W., Zorn M., Chang J. Y., Müllen K. and Zentel R., *Macromol. Rapid Commun.*, **30** (2009) 1179.
[4] Schmidt-Mende L., Fechtenkotter A., Müllen K., Moons E., Friend R. H. and MacKenzie J. D., *Science*, **293** (2001) 1119.
[5] Cisse L., Destruel P., Archambeau S., Seguy I., Jolinat P., Bock H. and Grelet E., *Chem. Phys. Lett.*, **476** (2009) 89.
[6] Grelet E. and Bock H., *Europhys. Lett.*, **73** (2006) 712.
[7] Pouzet E., De Cupere V., Heintz C., Andreasen J. W., Breiby D. W., Nielsen M. M., Viville P., Lazzaroni R., Gbabode G. and Geerts Y. H., *J. Phys. Chem. C*, **113** (2009) 14398.
[8] Thiebaut O., Bock H. and Grelet E., *J. Am. Chem. Soc.*, **132** (2010) 6886.
[9] Tang C. W., *Appl. Phys. Lett.*, **48** (1986) 183.
[10] Markovitsi D., Marguet S. and Bondkowski J., *J. Phys. Chem. B*, **105** (2001) 1299.
[11] Fujikake H., Murashige T., Sugibayashi M. and Ohta K., *Appl. Phys. Lett.*, **85** (2004) 3474.
[12] Charlet E., Grelet E., Brettes P., Bock H., Saadaoui H., Cisse L., Destruel P., Gherardi N. and Seguy I., *Appl. Phys. Lett.*, **92** (2008) 024107.
[13] De Cupere V., Tant J., Viville P., Lazzaroni R., Osikowicz W., Salaneck W. R. and Geerts Y. H., *Langmuir*, **22** (2006) 7798.
[14] Peumans P., Yakimov A. and Forrest S. R., *J. Appl. Phys.*, **93** (2003) 3693.
[15] Patel J. S. and Yokoyama H., *Nature*, **362** (1993) 525.
[16] Perova T. S., Vij J. K. and Kocot A., *Europhys. Lett.*, **44** (1998) 198.
[17] Nazarenko V. G., Boiko O. P., Park H.-S., Brodyn O. M., Omelchenko M. M., Tortora L., Nastishin Yu. A. and Lavrentovich O. D., *Phys. Rev. Lett.*, **105** (2010) 017801.
[18] Charlet E. and Grelet E., *Phys. Rev. E*, **78** (2008) 041707.
[19] Alibert-Fouet S., Dardel S., Bock H., Oukachmih M., Archambeau S., Seguy I., Jolinat P. and Destruel P., *ChemPhysChem*, **4** (2003) 983.
[20] Grelet E., Dardel S., Bock H., Goldmann M., Lacaze E. and Nallet F., *Eur. Phys. J. E*, **31** (2010) 343.
[21] Oswald P. and Pieranski P., *Smectic and Columnar Liquid Crystals: Concepts and Physical Properties Illustrated by Experiments* (Taylor and Francis/CRC Press, London) 2005.
[22] Oswald P., Malthete J. and Pelce P., *J. Phys. (Paris)*, **50** (1989) 2121.
[23] Oswald P., *J. Phys. (Paris)*, **49** (1988) 2119.
[24] Oswald P., *J. Phys. (Paris)*, **49** (1988) 1083.